M. P. Shaw P. R. Solomon

H. L. Grubin

## The Influence of Boundary Conditions on Current Instabilities in GaAs

**Abstract:** We obtain excellent agreement among experiments eliciting a variety of GaAs current instabilities and the results of a computer simulation of GaAs with various fields imposed at the cathode boundary. When the cathode field is below around 4 kV/cm theory and experiments show that the I-V characteristics of the active element are linear up to about 3 kV/cm where the current saturates and no transit-time oscillations occur. Experimentally this element gives rise to severe noise in a resistive circuit and sometimes tunable oscillations in a resonant circuit. When the cathode field is in the differential negative resistivity regime the I-V characteristics of the active element are nearly linear up to a threshold field (determined by the boundary field) where current drop, voltage rise and transit-time oscillations occur. For cathode fields above about 15 kV/cm the I-V characteristics are nonlinear and the element exhibits tunable oscillations in a resonant circuit.

During the past five years much work has been done to understand the electrical instabilities in GaAs. Although the published literature seems to have the problem well in hand, the situation in the laboratory remains chaotic. The usual approach has been to assume that samples with "good" contacts in "good" circuits yield the Gunn effect (or one of its variations) and that all other behavior can be blamed on "bad" circuits, "bad" material, or "bad" contacts. We propose a simple single parameter model which explains most of the observed behavior without recourse to such unproductive and misleading concepts.

The single parameter in the model is a fixed electric field imposed at the cathode boundary. We find that the cathode boundary field,  $E_c$ , controls the manifestation of the instability.  $^2$   $E_c$  determines whether the Gunn effect or another instability occurs. By assuming different values for  $E_c$  we simulate and systematically categorize the broad range of instabilities. The model is capable of predicting the details of the various instabilities and by comparing experiment with theory we can determine the carrier concentration and drift mobility of each sample.

The authors are located at the United Aircraft Research Laboratory in East Hartford, Connecticut 06108.

The model is based on the idea that metal-to-semiconductor junctions are inherently non-linear and are capable of supporting large electric fields. We assume the usual properties for the bulk GaAs and use the fixed cathode boundary field to simulate the effect of a low resistance junction. While a fixed cathode field is an oversimplification for the junction, the assumption has the essential features which allow us to systematically obtain all the instabilities by simply varying the magnitude of this field.

We have calculated, for various values of  $E_e$ , the current-voltage characteristics, electric field vs distance profiles, instability thresholds and current and voltage waveforms for samples situated in resistive and resonant circuits. The results are obtained by a computer simulation. We used the Butcher–Fawcett<sup>3</sup> results for the field-dependent diffusion coefficient and carrier velocity. We also assumed random doping fluctuations. The equation for the total current (assumed constant over a plane perpendicular to the direction of current) was solved simultaneously with the circuit equations.

The predictions of the model are shown in Fig. 1. For the same bulk characteristics we plot j vs  $\langle E \rangle$  (current density vs voltage/sample length) for four values of  $E_c$ . We superimpose the Butcher-Fawcett field dependent

587

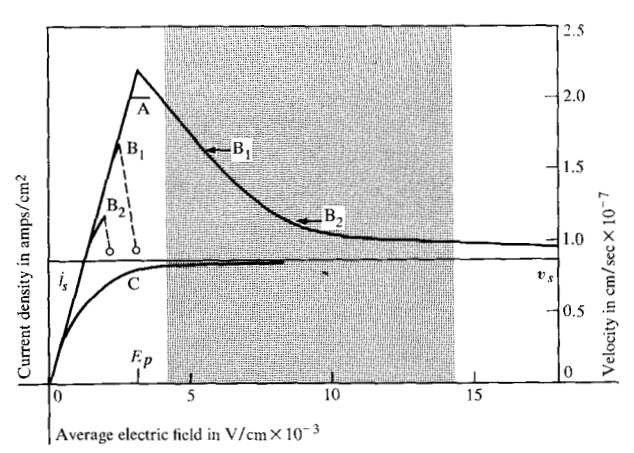


Figure 1 The v(E) curve and the computer simulated current density j as a function of average electric field  $\langle E \rangle$  (A through C) for various cathode boundary fields. The boundary field is zero for curve A, 24 kv/cm for curve C and is indicated by the arrow for curves  $B_1$  and  $B_2$ . The sample is  $10^{-2}$  cm long, has  $n=10^{15}$  cm<sup>-2</sup> and  $\mu=6,860$  cm<sup>2</sup>/V-sec. The right- and left-hand ordinates are related by j=nev.  $v_s=0.86\times 10^7$  cm/sec.

velocity curve, v(E). The manifestation of the instability can be divided into three categories. If  $E_c$  is in the shaded region, which contains most of the negative differential mobility range of the v(E) curve, then the instability appears as the classic Gunn effect. For lower or higher  $E_c$  other types of instabilities result. The Gunn effect occurs only for a specific range of boundary fields and is only one of several possible oscillatory modes.

For high  $E_c$  (curve C) the characteristic is linear only at low bias. At high bias the curve saturates at the current density  $j_* = nev_s$ . The departure from linearity corresponds to the appearance of a large cathode drop. The Gunn effect does not occur, but the sample sustains oscillations in a resonant circuit for a range of boundary fields and a range of applied voltages.

For  $E_e$  in the shaded region, the Gunn effect occurs (curves  $B_1$  and  $B_2$ ). Again, the departure from linearity is due to the appearance of a cathode drop. At threshold, the current switches along the load line. A very important point is that the threshold is controlled by  $E_e$  and is not at the peak of the v(E) curve. Threshold occurs before the bulk enters into the negative differential mobility regime. It occurs very near the current corresponding to the velocity  $v(E_e)$ . Therefore, the bulk threshold field can vary between 1.4 and 4.2 kV/cm for mobilities between 4000 and 7000 cm<sup>2</sup>/V-sec.

For low  $E_c$  (curve A) the  $j-\langle E \rangle$  curve is essentially linear almost up to the field at peak velocity,  $E_p$ . At this point several things may occur. The possibilities depend in a detailed way on the characteristics of the GaAs and the circuit. Domains may be nucleated at large doping fluctuations in the bulk leading to large "peak-to-valley"

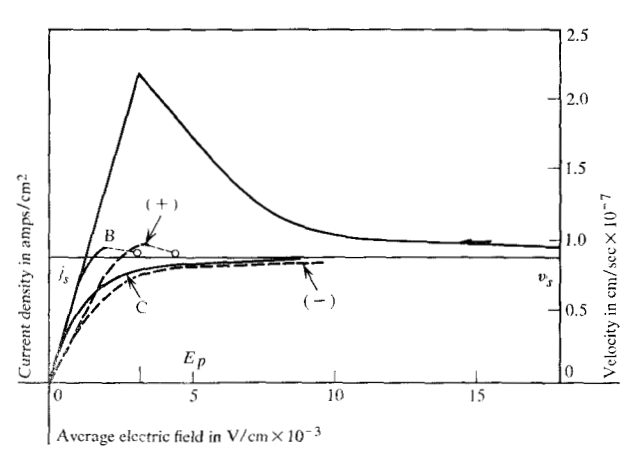


Figure 2 Experimental  $j-\langle E\rangle$  curves (+) and (-) (dashed) and theoretical curves B and C (solid). The only significance in the fact that the low field slopes differ is that the theoretical curve is for a mobility of 6,860 cm<sup>2</sup>/V-sec, whereas the experimental curve is for a mobility of 4000 cm<sup>2</sup>/V-sec.

ratio transit-time oscillations. A more interesting possibility is that after a domain (nucleated in the bulk) reaches the anode it may remain there in a stationary field configuration and the current will saturate. In a resonant circuit the bulk field may oscillate at the resonant frequency. Switching may also take place between possible modes with changes in bias.

We have experimentally investigated a large number of GaAs samples of various mobilities (3000 to 7000  $\rm cm^2/V$ -sec) and room temperature carrier concentration (3  $\times$  10<sup>14</sup> to 10<sup>16</sup> cm<sup>-3</sup>). We varied the contacting procedures and made measurements in a variety of circuits. We measured the current-voltage characteristics, probed the potential distributions and observed the current and voltage waveforms. We observed a broad spectrum of characteristics and behavior, almost all of which are consistent with the model. We have also examined the literature and find the model to be consistent with the reported results, including those termed anomalous.

Space is insufficient for a detailed comparison of theory and experiment, so we have picked an example to demonstrate the important point that the cathode boundary field controls the nature of the instability. In this case we have made the same GaAs bulk exhibit instabilities in the high, intermediate, and low boundary field regimes. The sample was made from Monsanto n-GaAs having a nominal carrier concentration of  $10^{15}$  cm<sup>-3</sup> and Hall mobility of 4700 cm<sup>2</sup>/V-sec. Figure 2 shows experimental  $j-\langle E\rangle$  characteristics (dashed) normalized to the v(E) curve in a manner which we will discuss. The experimental curves represent both voltage polarities and are to be compared with the predicted curves (solid lines). The

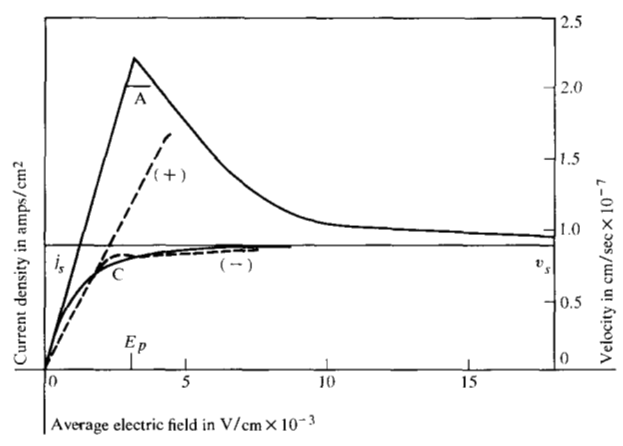


Figure 3 Experimental  $j-\langle E \rangle$  curves (+) and (-) (dashed) taken after sculpturing the sample in Fig. 2 and theoretical curves A and C (solid).

unknown boundary fields are picked to produce the best fit with experiment. Comparison of the theoretical and experimental curves indicates that the large asymmetry in the experimental curves is due to the asymmetry (which need not be large) of the fields at the cathode boundary. For the (+) direction a departure from linearity appears (corresponding to a measured cathode drop) and a Gunn effect with small peak-to-valley ratio occurs. For the saturating direction (-) a very large cathode drop appears. The fact that a large cathode drop appears for the (-) polarity while no anode drop appears for the (+) polarity shows that the contacts are asymmetric junctions. For the (-) polarity the sample is stable in a resistive circuit but sustains oscillations in a resonant circuit over the investigated range from 0.1 to 8.2 GHz.

In order to make the sample exhibit the characteristics of bulk GaAs with low field boundaries we reduced the cross-sectional area (by a factor of  $\approx$ 10) over a region between one contact and a point midway between the contacts. The reduced region becomes the active element of the bulk. We have removed the active region from the influence of one of the junctions. Figure 3 shows the new characteristics obtained after cutting. The (-) j- $\langle E \rangle$  curve is for the case when the reduced contact was the cathode and is similar to the (-) curve before cutting.

Significantly different behavior was observed when the large contact was the cathode. In this case the boundary of the active region was controlled not by the high field at the junction but by the much lower field at the plane where the cross-sectional area changes. Here the j-E characteristic (+) is nearly linear almost up to the peak current where it saturates, without a current drop. The results are in good agreement with the predicted curves.

Experimental observations on samples with reduced cross-sections of various shapes and sizes are in reasonable

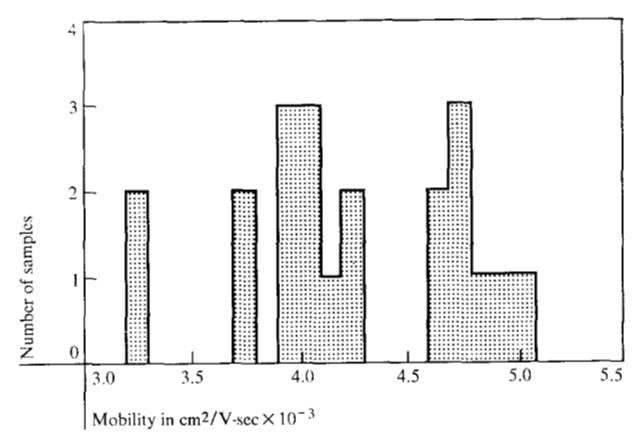


Figure 4 Histogram of mobilities measured according to the model.

agreement with the predicted possibilities. We have observed domain nucleation in the bulk, stable high fields at the anode, and switching between the transit time and high anode field state as a function of bias. Most important is that individual sculptured samples have sustained oscillations in resonant circuits over the investigated range from 0.1 to 8.2 GHz.

The agreement between experiment and theory is sufficiently close to warrant use of the model to determine the carrier concentration and drift mobility in individual samples. For small samples these parameters are very difficult to obtain by more conventional means. For example, for high  $E_c$  the computed results indicate that the current saturates when the average carrier velocity is  $v_s$ . To obtain the carrier concentration n we measure  $j_s$  and assume  $n = j_s/ev_s$ , where for  $v_s$  at room temperature we take the theoretical value  $0.86 \times 10^7$  cm/sec. We normalize the j-E curves to the v(E) curve by using these values of n. We determine the low-field drift mobility  $\mu$  by using n and the measured resistivities. Figure 4 is a mobility histogram for several samples cut from two slices taken from two different Monsanto crystals. The confinement of the mobility to the expected range is justification for assuming that the prediction  $j_s =$ nev, is valid.

We have also examined the temperature dependence of  $j_*$ . Data are shown in Fig. 5 for a typical sample. We plot  $j_*$ , which we assume to be equal to  $nev_*$ , vs the conductivity  $\sigma(=ne\mu)$  for the temperature range 178°K to 351°K. The figure contains a line of unit slope which passes through the room temperature datum point. The other data points would lie on this line if  $\mu$  and  $v_*$  were temperature independent. The closeness of the data points to the line of unit slope is further justification for the assumption  $j_* = nev_*$ . The departure from the straight line is probably due to the temperature depend-

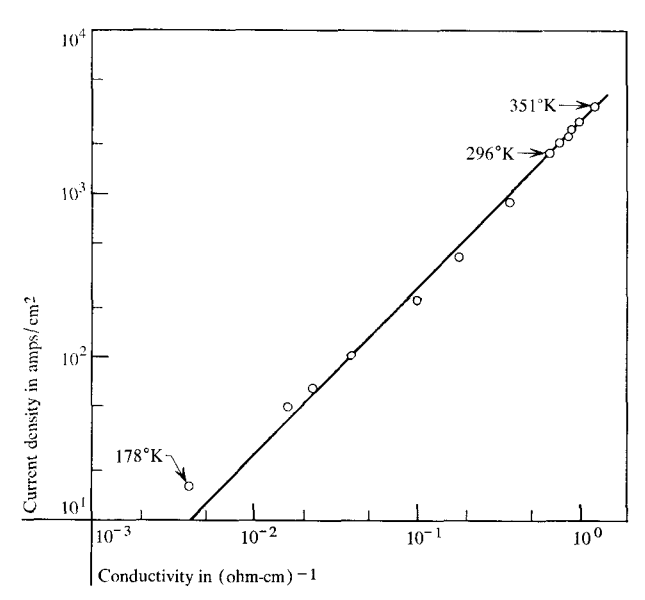


Figure 5 Saturated current density as a function of conductivity.

ence of  $v_s$ . For a constant mobility equal to the value computed at room temperature  $v_s$  ranges from  $1.5 \times 10^7$  cm/sec at  $178^{\circ}$ K to  $0.9 \times 10^7$  cm/sec at  $351^{\circ}$ K. The results are in reasonable agreement with the results of Ruch and Kino.<sup>4</sup>

We have demonstrated that it is possible, by emphasizing the critical role played by the electric field at the cathode boundary, to develop a simple model which

provides a basis for understanding almost all of the observed instabilities. Recognition that the electric field at the boundary is the principle determinant of the instability makes possible the understanding of the various modes without resorting to such concepts as "good" or "bad" contacts. The model also provides a framework within which one can categorize and characterize the various modes. Within subcategories, such as the Gunn effect, the model provides a satisfactory way of looking at a particular phenomenon, such as the instability threshold, and enables us to understand why it has been difficult in the past to understand these phenomena only in terms of bulk material parameters. The good agreement between experiment and theory now makes it possible to use the results of the model to determine the carrier density and drift mobility of each sample.

## References

- The propagation of a high field domain from cathode to anode. See, e.g., J. B. Gunn, IBM J Res. Develop. 8, 141 (1964), 10, 300 (1966), 10, 310 (1966).
- The importance of the boundary conditions in predicting the behavior of nonlinear semiconductors has been realized and exploited by Böer, see, e.g., K. W. Böer et al., Phys. Rev. 169-3, 700 (1968), 171-3, 899 (1968); Phys. Stat. Sol. 30, 291 (1968). See also H. Kroemer, IEEE Trans. Electron Devices ED-15, 819 (1968), and D. E. McCumber, J. Phys. Soc. Japan 21, 522, Suppl. (1966).
- 3. P. N. Butcher, Rpts. Prog. Phys. 30, 97 (1967)
- 4. J. G. Ruch and G. S. Kino, Phys. Rev. 174, 921 (1968).

Received April 9, 1969